Supporting Information

Scapini et al. 10.1073/pnas.1107913108

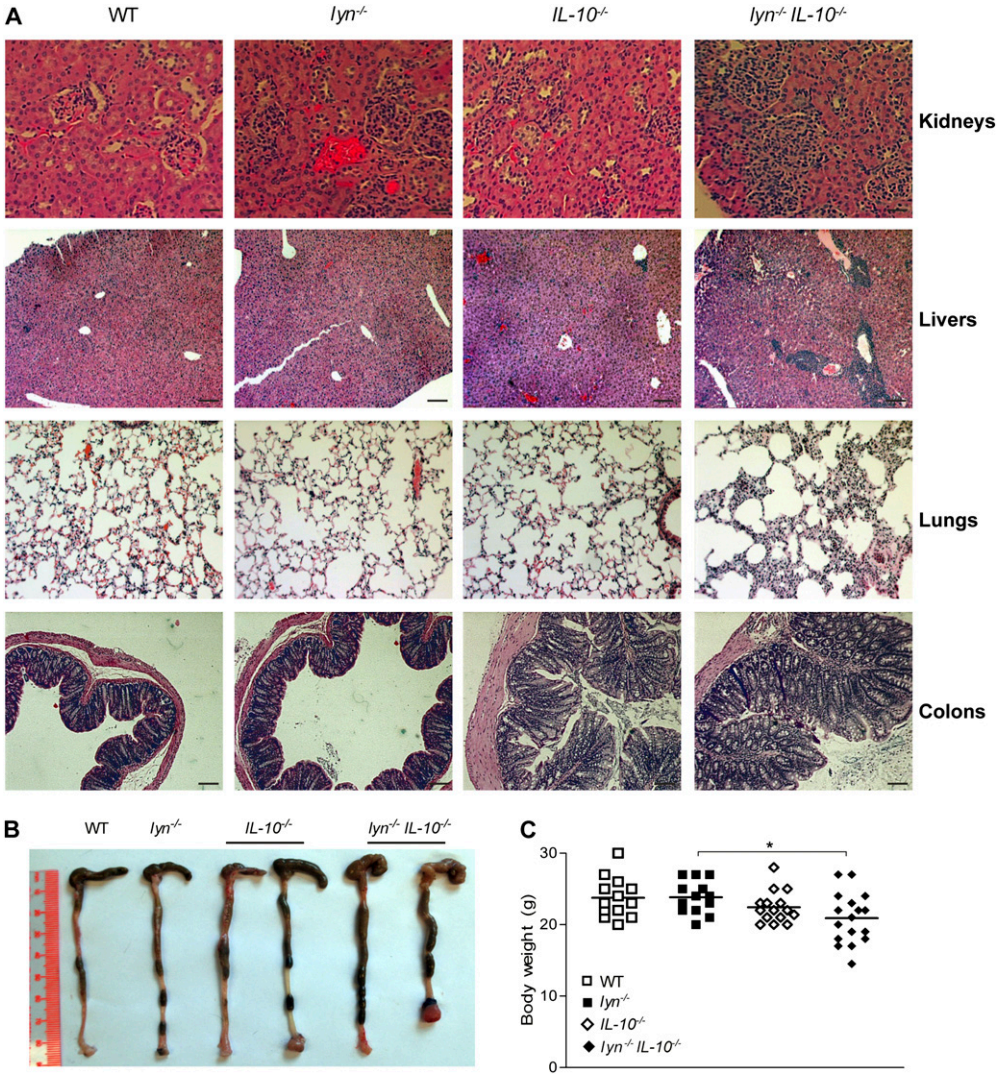

Fig. S1. IL-10 deficiency exacerbates tissue inflammation in $lyn^{-/-}$ mice. (*A*) Representative H&E staining of kidneys (magnification: ×200; top row), livers (magnification: ×100; second row), lungs (magnification: ×100; third row), and colons (magnification: ×100; bottom row) sections from 5- to 6-mo-old WT, $lyn^{-/-}$, $IL\text{-}10^{-/-}$, or $lyn^{-/-}IL\text{-}10^{-/-}$ mice. (Scale bars: *A*, 200 μm.) Data are representative of 10 to 12 mice for each genotype analyzed at end-point experiments. (*B*) Representative images of colons from 5- to 6-mo-old WT, $lyn^{-/-}$, $IL\text{-}10^{-/-}$, or $lyn^{-/-}IL\text{-}10^{-/-}$ mice. Data are representative of 10 to 12 mice for each genotype analyzed at end-point experiments. (*C*) Each symbol represents the body weight of an individual 5- to 6-mo-old WT, $lyn^{-/-}$, $IL\text{-}10^{-/-}$, or $lyn^{-/-}IL\text{-}10^{-/-}$ mouse. Data are pooled from three independent end-point experiments. Statistical differences of $lyn^{-/-}IL\text{-}10^{-/-}$ double-mutant vs. $lyn^{-/-}$ or $IL\text{-}10^{-/-}$ single-mutant mice are reported ($*P < 0.05$).

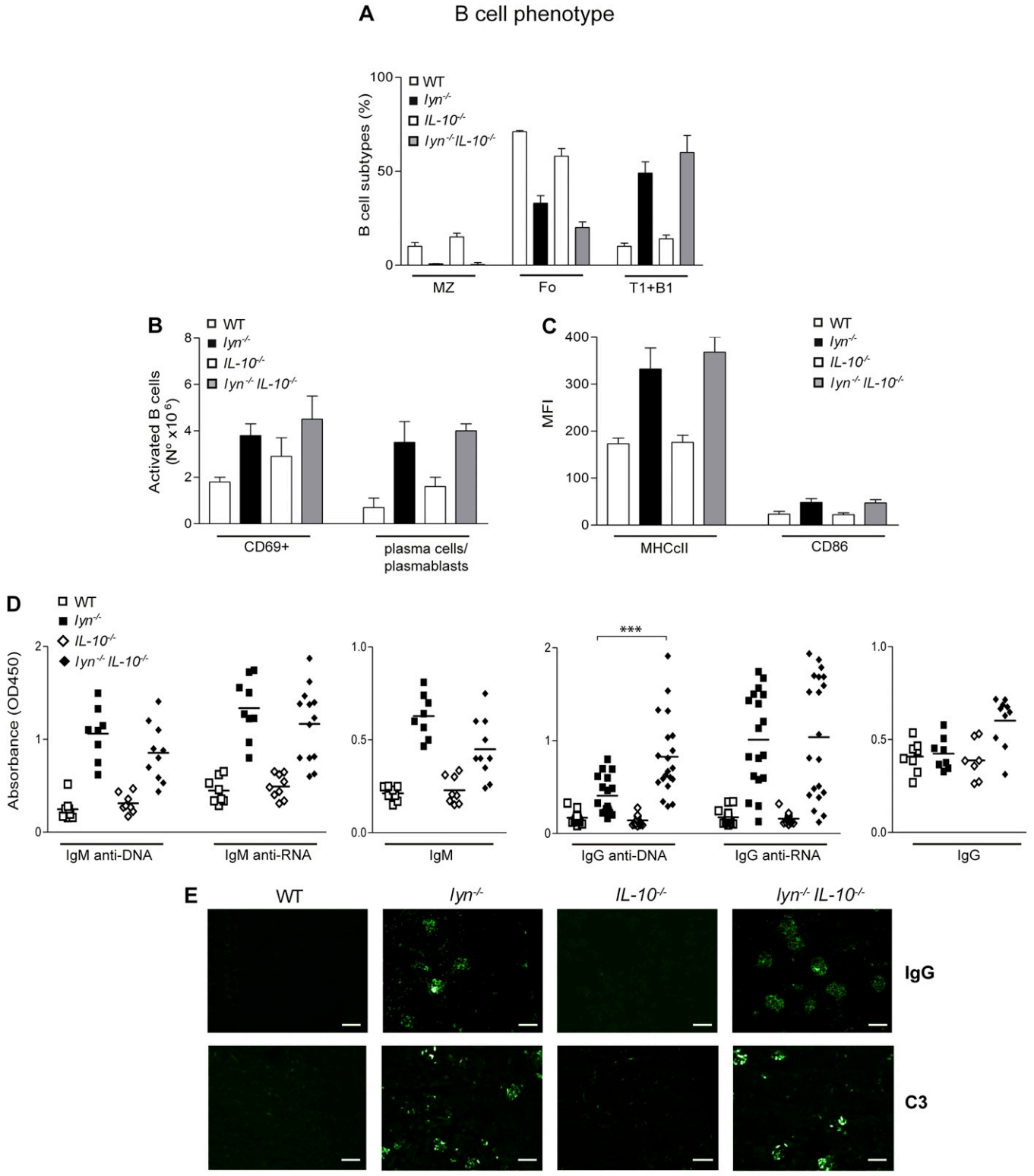

Fig. S2. IL-10 deficiency does not affect the B-cell phenotype, activation, and immune complex/C3 deposits in the kidneys in $lyn^{-/-}$ mice. (*A–C*) Single-cell suspensions of spleens were prepared from 5- to 6-mo-old WT, $lyn^{-/-}$, $IL\text{-}10^{-/-}$, and $lyn^{-/-}IL\text{-}10^{-/-}$ mice. The percentage of MZ B cells ($CD19^{+}CD21/CD35^{high}CD23^{-}$), Fo B cells ($CD19^{+}CD21/CD35^{int}CD23^{+}$), and transitional T1 B cells + B1 cells (T1+B1; $CD19^{+}CD21/CD35^{-}CD23^{-}$) (*A*), the absolute number of $CD19^{+}CD69^{+}$ and $CD19/B220^{low/-}CD138^{+}$ (plasma cells/plasmablasts) (*B*), and the MFI of MHCcII and CD86 (B7-2) expression of $CD19^{+}$ cells (*C*) were determined by flow cytometric analysis. Data are representative of two end-point experiments and are presented as mean ± SEM (n = 8–10 mice per group). (*D*) Each symbol represents the serum levels of IgM specific to DNA or RNA or total (two left graphs) and IgG specific to DNA or RNA or total (two right graphs) present in individual 5- to 6-mo-old WT, $lyn^{-/-}$, $IL\text{-}10^{-/-}$, or $lyn^{-/-}IL\text{-}10^{-/-}$ mice, assessed by ELISA. Data are pooled from two independent end-point experiments. (*E*) Kidneys were collected and tissue was frozen for immunofluorescence staining of IgG immune complex and C3 deposits. Representative IgG (*Upper*) and C3 (*Lower*) staining of kidneys from 5- to 6-mo-old WT, $lyn^{-/-}$, $IL\text{-}10^{-/-}$, and $lyn^{-/-}IL\text{-}10^{-/-}$ mice (magnification: ×200). (Scale bars: 100 μm.) Data are representative of eight to 10 mice for each genotype analyzed at end-point experiments.

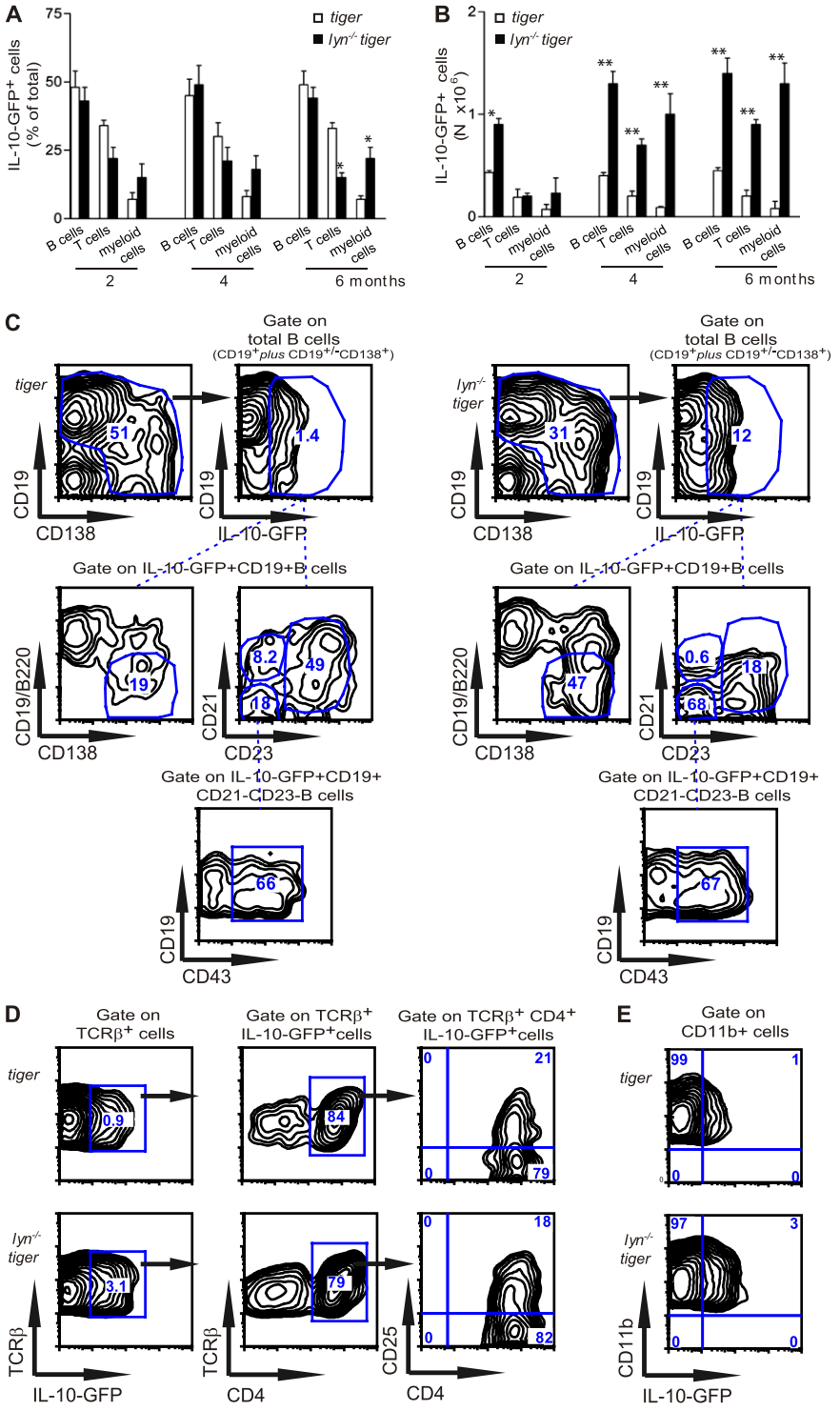

Fig. S3. Phenotype of IL-10–GFP$^+$ cells in control *tiger* and *lyn*$^{-/-}$*tiger* mice. Single-cell suspensions of spleens from control *tiger* or *lyn*$^{-/-}$*tiger* mice were stained for flow cytometric analysis. The gates designed to analyze GFP expression were set by using regular WT or *lyn*$^{-/-}$mice as GFP$^-$ controls. (*A*) The frequency of total IL-10–GFP$^+$ cells (among total splenic population) in 2- to 6-mo-old control *tiger* or *lyn*$^{-/-}$*tiger* mice is reported. Data are pooled from two separate experiments and are presented as mean ± SEM (n = 6–8 mice per group). (*B*) The total number of IL-10–GFP$^+$ B cells (among total CD19$^+$ *plus* CD19/B220$^{low/-}$CD138$^+$ cells), IL-10-GFP$^+$ T cells (among total TCRβ$^+$ cells), and IL-10–GFP$^+$ myeloid cells (among total CD11b$^+$ cells) in 2- to 6-mo-old *tiger* and *lyn*$^{-/-}$*tiger* mice are reported. Data are pooled from two separate time-course experiments and are presented as mean ± SEM (n = 6–8 mice per group). Statistical differences of *lyn*$^{-/-}$*tiger* vs. control *tiger* mice are reported (*P < 0.05; **P < 0.01). (*C*) Representative flow plots show the frequency (among total CD19$^+$ *plus* CD19/B220$^{low/-}$CD138$^+$ cells) and the phenotype (expression levels of CD138, CD21, CD23, and CD43) of IL-10–GFP$^+$ B cells in the spleen of 2-mo-old control *tiger* or *lyn*$^{-/-}$*tiger* mice. Data are representative of five or six mice for each genotype. (*D*) Representative flow plots show the frequency (among total TCRβ$^+$ T-cell population; *Left*) and phenotype (expression of CD4, *Center*; and CD25, *Right*) of IL-10–GFP$^+$ T cells in the spleen of 2-mo-old control *tiger* or *lyn*$^{-/-}$*tiger* mice. (*E*) Representative FACS plots show the frequency (among total CD11b$^+$ myeloid cell population) of IL-10–GFP$^+$ myeloid cells in the spleen of 2- mo-old control *tiger* or *lyn*$^{-/-}$*tiger* mice. Data are representative of five or six mice for each genotype.

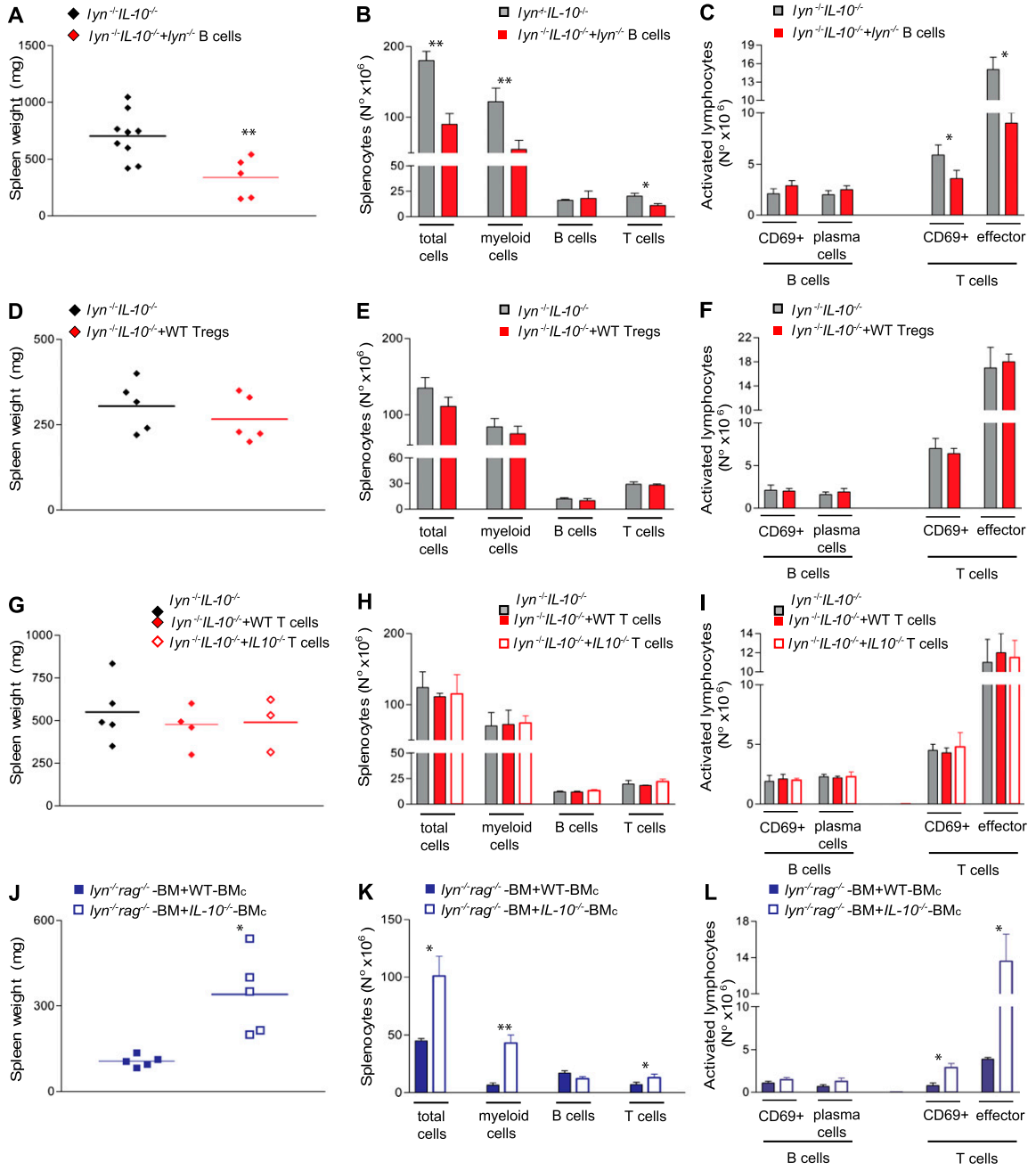

Fig. S4. IL-10 production by $lyn^{-/-}$ B cells is sufficient to reduce the disease development in $lyn^{-/-}IL\text{-}10^{-/-}$ mice, whereas IL-10 production by $CD4^+$ Tregs, total T cells, or myeloid cells is not sufficient to reduce disease. (*A–I*) Two-month-old $Lyn^{-/-}IL\text{-}10^{-/-}$ chimeras were injected with 5×10^6 $CD19^+$ $lyn^{-/-}$ B cells (isolated from spleen and lymph nodes of 2-mo-old $lyn^{-/-}$ animals; *A–C*), 10×10^6 WT $CD4^+$ Tregs (isolated and expanded in vitro; *D–F*), or WT or $IL\text{-}10^{-/-}$ T cells (10×10^6 $TCR\beta^+$ T cells, isolated from spleen and lymph nodes of 2-mo-old WT or $IL\text{-}10^{-/-}$ animals; *G–I*). Two to 3 mo after the adoptive transfer, recipient $lyn^{-/-}IL\text{-}10^{-/-}$ mice were killed and analyzed for signs of disease development. (*J–L*) Chimeric mice were generated by reconstituting the hematopoietic system of lethally irradiated WT or $IL\text{-}10^{-/-}$ animals with bone marrow from $lyn^{-/-}rag^{-/-}$ mice mixed, in a ratio of 75% to 25%, with WT or $IL\text{-}10^{-/-}$ bone marrow. Four months after reconstitution, the mixed chimeras were killed and analyzed for signs of disease development. Each symbol represents the weight of an individual mouse spleen. The absolute number of total, myeloid ($CD11b^+$), total B ($CD19^+$ plus $CD19/B220^{low/-}CD138^+$ cells), and T ($TCR\beta^+$) cells is reported. T effectors are defined as $TCR\beta{+}CD44^{high}CD62L^-$, whereas plasma cells/plasmablasts were $CD19/B220^{low/-}CD138^+$. Data were pooled from two independent end-point experiments and are presented ± SEM (n = 5–9 mice per group; $^*P < 0.05$; $^{**}P < 0.01$).